Angle-dependent spectrum measurement of polystyrene opal-like structure described by Bragg-Snell diffraction and perturbed photonic band structure

N Sitpathom[1*], T Muangnapoh[2], P Kumnorkaew[2], S Suwanna[1], A Sinsarp[1] and T Osotchan[1]

[1] Department of Physics, Faculty of Science, Mahidol University, Bangkok 10400, Thailand
[2] National Nanotechnology Center (NANOTEC), National Science and Technology Development Agency, Pathum Thani 12120, Thailand

*E-mail: nonthanan.sit@student.mahidol.ac.th

Abstract. Optical diffraction of opal structure, a colloidal photonic crystal, can be predicted by Bragg-Snell diffraction and photonic band structure. Theoretical prediction and optical measurement are frequently slightly different due to distance variation of particle packing. In this research, opal of 310 nm polystyrene beads was fabricated by self-assembly process and optically investigated in transmission spectra at varied angles. The measured spectra had less agreement to the Bragg-Snell prediction at large angle of detection. To explore influence of packing distance on optical response, photonic band structures were numerically simulated via plane-wave expansion method at presence of perturbed length in primitive lattice vectors. Extending each primitive vector with fixing others provided a different eigen-frequency of the first photonic band, although they had a symmetrical perturbation on (111) face-centered cubic. Perturbation on lattice length became much strong when the disturbing direction was out of eigenstate orientation plane.

1. Introduction

Optical diffraction of colloidal photonic crystals, frequently called as opals, can be well predicted by Bragg-Snell prediction [1] in some regions. The Bragg-Snell equation combines between diffraction of parallel crystal planes (Bragg's diffraction) and refraction at interface of two media (Snell's law) with various incidence angle. The Bragg-Snell equation from (111) surface can be written in general form for (hkl) plane diffraction as

$$\lambda_{(hkl)}(\theta) = 2d_{(111)}n_{eff}\left(\frac{3}{h^2+k^2+l^2}\right)^{1/2}\cos(\theta - \Psi_{(hkl)}) . \quad (1)$$

The diffracted wavelength $\lambda_{(hkl)}$ from (hkl) plane at incidence angle θ is calculated from the product of (111) d-spacing, effective refractive index n_{eff} and cosine of relative angle of (111) and (hkl) planes $\Psi_{(hkl)}$. There were several reports that the measured Bragg diffraction angles can be differ from the theoretical prediction values [2-3]. Moreover, the diffraction intensity becomes weaker in disordered opal and its peak slightly shifts to longer wavelength [4-5]. The main cause of disordered opal was

assumed by variation of particle diameters, thermal fluctuation in self-assembly process [6] and solution evaporation rate [7]. For face-centered cubic (fcc) structure of opal, anti-band crossing of (111) to (200) and $(\bar{1}11)$ was observed at 30° for U and K symmetry points, respectively, and at 40° in the orthogonal axis for W symmetry point [8].

Fabrication of opals is easily made by self-assembly process of colloidal packing with natural forces such as capillary and Van der Waals forces [9]. For solution process, a convective deposition is a well-alternative approach among the others for example spin coting, dip coating or vertical deposition [9]. In order to obtain better crystal quality, the convective deposition can achieve by using substrate vibration during coating [10].

In this work, the convective deposition with vibration assistance was used for opal film fabrication. Opal microstructure was observed by scanning electron microscope (SEM) and the self-assembled opals were optically characterized by transmission spectra at varied angles. Moreover, an imperfection of opal structures was computationally studied via plane-wave expansion method (PWEM).

2. Experiment and simulation methods

The fcc structures of polystyrene particles (purchased from Thermo Fisher Scientific) with diameter of 310±9 nm (standard deviation < 3%) were prepared by convective deposition [11]. The glass substrate was moved with speed of 10 μm/s by linear motor and vibrated at frequency of 40 Hz during self-assemble process. The microstructure of fabricated opal films were observed by SEM with conductive ultrathin film coating.

For optical characterization, the transmission spectra were examined for investing Bragg diffraction and analyzing opal crystal quality. The transmission measurement was performed in Shimadzu UV-Vis 2600 spectrometer with varying the sample angle from -50° to 0° and 0° to +50° with respect to normal axis of the substrate.

The photonic band structures and their related electric fields were studied on varied perturbation axes by PWEM which is having eigenfrequencies and eigenstates by solving Maxwell's eigen-equation. The simulation was performed by MIT Photonic Bands (MPB), open-source software. The primitive vectors and high symmetry points used in this PWEM simulation were taken from reference [12]. Three primitive vectors of fcc were defined as $\mathbf{a_1}$, $\mathbf{a_2}$ and $\mathbf{a_3}$ for $(0,1/2,1/2)$, $(1/2,0,1/2)$ and $(1/2,1/2,0)$, respectively. To study photonic bandgap change under perturbed lattice, the translation vector along each primitive vector was extended by 10%. Thus, the sets of imposed perturbed vectors were $(1.1\mathbf{a_1},1.0\mathbf{a}_2,1.0\mathbf{a}_3)$, $(1.0\mathbf{a_1},1.1\mathbf{a}_2,1.0\mathbf{a}_3)$ and $(1.0\mathbf{a_1},1.0\mathbf{a}_2,1.1\mathbf{a}_3)$.

3. Results and discussion

The opal film of 310 nm polystyrene particles presented violet color as shown in figure 1 (a). The opal structure showed hexagonal layer packing as observed by SEM (figure 1 (b)). There are multi-domain orientations of the order particles and small areas of disorder particle' assembly at grain boundaries. Multiple domains in self-assembly can be caused by fast evaporation rate of solution and simultaneous crystal formation in different places [7]. Moreover, the variation in thermal gradient in solution and hydrophilicity of substrate surface [6] would induce point and line defects in opal film.

Transmission spectra of the 310 nm opal films were measured at -50° to 0° and 0° to 50° with 5° increment and plotted in figure 1 (c). Predicted-diffracted wavelengths estimated by Bragg- Snell equation were labelled on the spectra by black, red and green arrows for (111), (200) and $(\bar{1}11)$ plan of fcc, respectively. The measured spectra and the estimated diffraction peaks had well agreement in the region where the angles varied between -20° to 0° to +20° and became different for the wider angles. This may occur due to a higher chance of multi-domain measurement at large angle with larger projection area. Additionally, the diffraction peaks merging of (111) and $(\bar{1}11)$ planes at angle of about 25° can be another factor of the shift [2]. The misaligned stacking sequence of particle layers can disturb the opal crystal structure and can result in variation of packing period.

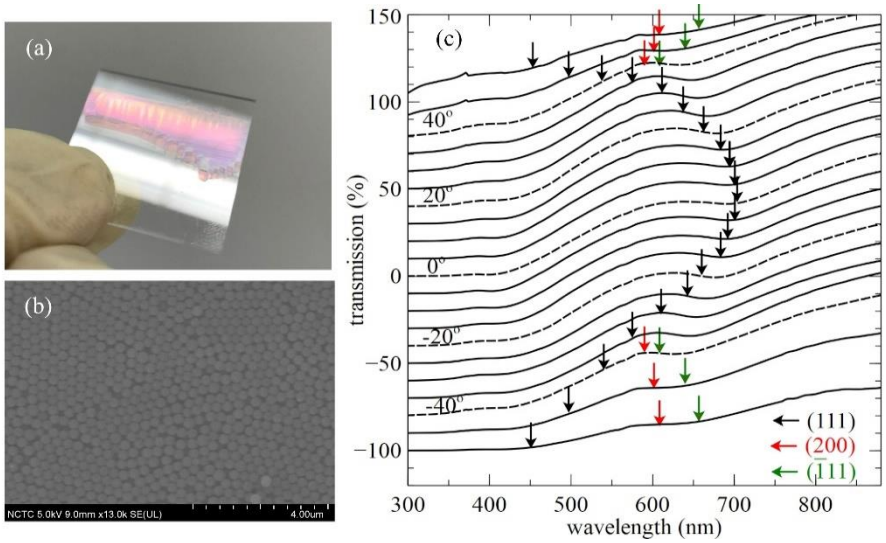

Figure 1. (a) Photograph of fabricated opal film presenting violet color, (b) SEM image of order 310 nm nanoparticle opal film and (c) transmission spectra measured at angles from -50° to 0° to +50° with black, red, and green arrows labelled of predicted diffraction wavelength from (111), (200) and $(\bar{1}11)$ fcc planes, respectively.

Simulation of eigen electric fields on photonic band structures was applied to explore the effect of perturbed lattice distance on photonic band gap. The lower band-edge of the first bandgap in ΓL direction, corresponding to [111] fcc, indicated strong effect for the case of perturbation vector $\left(1.0\mathbf{a_1}, 1.1\mathbf{a}_2, 1.0\mathbf{a}_3\right)$, see the circle in figure 2 (b). For electric-field energy density of this perturbation axis, the mode field was spatially spanned out of plane, while those in the other cases were extended in plane. Although three primitive vectors had the same projected angle to vector $[111]$, only the perturbed $\mathbf{a_2}$ direction case had the most influence on the first photonic bandgap due to pointing out to the plane of field localization direction. Additionally, the spatial shape of electrical energy localization become more spherical at the $\mathbf{a_2}$ perturbation, see color contours figure 3. Having optical localization in different geometrical shape would be a reason of shifted eigenfrequency.

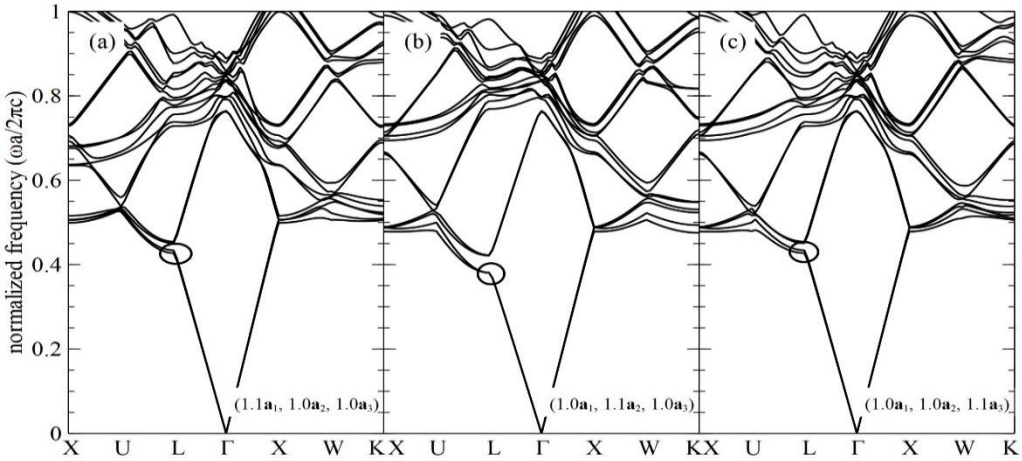

Figure 2. Photonic band structures of perturbed opal crystals with primitive vectors of (a) $(1.1\,\mathbf{a_1}, 1.0\,\mathbf{a_2}, 1.0\,\mathbf{a_3})$, (b) $(1.0\,\mathbf{a_1}, 1.1\,\mathbf{a_2}, 1.0\,\mathbf{a_3})$ and (c) $(1.0\,\mathbf{a_1}, 1.0\,\mathbf{a_2}, 1.1\,\mathbf{a_3})$.

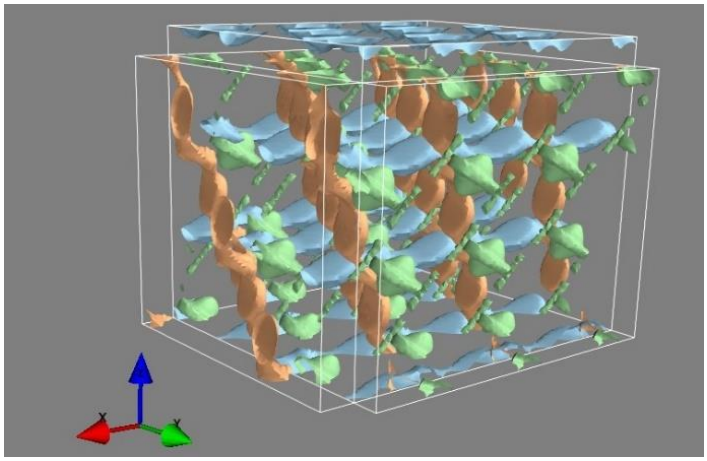

Figure 3. Contours of electric-field energy density fixing the value at 3.5 shown in blue, green and red colors for perturbation on $\mathbf{a}_1$, $\mathbf{a}_2$ and $\mathbf{a}_3$, respectively. The x-, y- and z-axis presented in red, green and blue arrows.

4. Conclusion

Colloidal photonic crystals or opal structures was fabricated by convective deposition with vibration assistance and exhibits optical diffraction predicted by Bragg-Snell equation. The measured diffracted wavelengths have some agreement to the theoretical prediction in region of low angle of incidence but the shift occurred at large angle probably due to several grains involving at this large projection area of incidence and non-ideal face-centered cubic packing. For simulation by plane-wave expansion method, the perturbation effect on photonic bandgap became strong for the perturbed crystal with Eigen electric field mode extending in out of localization plane.

Acknowledgments

The first author would like to thanks the Thailand Development and Promotion of Science and Technology Talent Program for a scholarship. This project was partially supported by the Research Nanotechnology Network (RNN), National Nanotechnology Center.

References

[1] Baryshev A V, Kaplyanskiĭ A A, Kosobukin V A, Limonov M F and Skvortsov A P 2004 *Phys. Solid State* **46** 1331–9

[2] Baryshev A V, Khanikaev A B, Uchida H and Inoue M 2006 *Phys. Rev.* B **73** 033103

[3] Omshankar, Priya and Nair R V 2019 *J. Opt. Soc. Am.* B **36** 2338–45

[4] Palacios-Lidón E, Juárez B H, Castillo-Martínez E and López C 2005 *J. Appl. Phys.* **97** 063502

[5] Rengarajan R, Mittleman D, Rich C and Colvin V 2005 *Phys. Rev.* E **71** 016615

[6] Boettcher J M, Joy M, Joshi K, Muangnapoh T and Gilchrist J F 2015 *Langmuir* **31** 10935–8

[7] Cheng S and Grest G S 2013 *J. Chem. Phys.* **138** 064701

[8] Rybin M V, Samusev K B and Limonov M F 2007 *Photonics Nanostructures: Fundam. Appl.* **5** 119–24

[9] Vogel N, Retsch M, Fustin C-A, del Campo A and Jonas U 2015 *Chem. Rev.* **115** 6265–311

[10] Joy M, Muangnapoh T, Snyder M A and Gilchrist J F 2015 *Soft Matter* **11** 7092

[11] Sitpathom N, Kumnorkaew P, Muangnapoh T, Rutirawut T and Osotchan T 2017 *Materials Today: Proc.* **4** 6485–90

[12] Setyawan W and Curtarolo S 2010 *Comput. Mater. Sci.* **49** 299–312